

Comparison of Crystal Structure, Surface Morphology Structure, and Energy Band Gap of Thin Films of Zinc Oxide, Tin(IV) Oxide, and Titanium Dioxide

Teguh Ardianto^{1*}, Aris Doyan², Susilawati², Dedi Riyan Rizaldi³, Ziadatul Fatimah⁴, Muhammad Ikhsan⁵ and Nuraini Rachma Ardianti⁵

¹Physics, Faculty of Mathematics and Science, University of Mataram, Jl. Majapahit No. 62 Mataram 83125, Indonesia

²Physics Education, Faculty of Teacher Training and Education, University of Mataram, Jl. Majapahit No. 62 Mataram 83125, Indonesia

³MA Plus Nurul Islam Sekarbela, Jl. Swasembada No. IX Karang Pule Mataram 83115, Indonesia

⁴SMA NW Mataram, Jl. Kaktus No. 1-3 Mataram 83126, Indonesia

⁵Balai Publikasi Indonesia, Jl. Pendidikan No. 37 Mataram 83125, Indonesia

ABSTRACT

This study was conducted with the aim of analyzing the crystal structure, surface morphology structure, and energy band gap values in zinc oxide (ZnO), tin(IV) oxide (SnO₂), and titanium dioxide (TiO₂) thin films. This study uses an experimental research type that goes through two stages of work, namely synthesis and characterization of thin films. The synthesis stage is through the process of making sol-gel solutions, depositing solutions on substrate media, and heating thin film samples. While the characterization stage is carried out through three testing processes using X-ray diffraction (XRD), scanning electron microscopy (SEM), and UV-Vis spectrophotometry. The research data obtained were analyzed descriptively and presented in the form of images, tables, and graphs to see the quality and characteristics of the test samples. Based on the results of the analysis, it is known that the crystal structure of the ZnO thin film is hexagonal while SnO₂ and TiO₂ are tetragonal. The surface morphology of the SnO₂ and TiO₂ thin films is granular, while the ZnO thin

film is a nanorod. The smallest energy band gap value is found in the ZnO thin film with a value of 2.00 eV. There are four factors that affect the energy band gap value in thin films, namely precursor material, deposition method, substrate media, and dopant material.

Keywords: Crystal structure, energy band gap, morphological structure, thin film, tin(IV)oxide, titanium dioxide, zinc oxide

ARTICLE INFO

Article history:

Received: 15 December 2024

Accepted: 17 March 2025

Published: 23 July 2025

DOI: <https://doi.org/10.47836/pjst.33.4.15>

E-mail addresses:

teguhardianto@unram.ac.id (Teguh Ardianto)

aris_doyan@unram.ac.id (Aris Doyan)

susilawatihambali@unram.ac.id (Susilawati)

dedi0313@gmail.com (Dedi Riyan Rizaldi)

ziadatulfatihmah96@gmail.com (Ziadatul Fatimah)

muhammadikhsan99.mi@gmail.com (Muhammad Ikhsan)

nurainirachmaa@gmail.com (Nuraini Rachma Ardianti)

* Corresponding author

INTRODUCTION

Researchers worldwide have paid considerable attention to the development of technology in the field of materials. Various studies have been conducted with the aim of producing materials that have good characteristics and are in accordance with human needs. One way that can be done to produce materials that are in accordance with what is desired is by using the material coating technique process (Butt, 2022). In today's conditions, various material coating sciences and technologies play a very important role in the electronics industry. One of the main objectives of this development process is to be able to meet the various needs for a circuit that is integrated and often used in the electronics industry process (McIvor & Humphreys, 2004). Research on material coatings that is often carried out today is the process of forming thin layers.

A thin layer is a layer on a material that has a thickness ranging from nanometers (single layer) to micrometers (Koziej et al., 2014). This thickness condition when compared to the substrate used is included in the very thin category. Currently, thin films are of interest to develop because they can impart new properties to materials. Thin films have characteristics such as a uniform surface (coating the substrate evenly without defects), stable surface temperature and high precision, strong intermolecular adhesion, and crystal structure (Zhao et al., 2008). Thin layers can be developed by carrying out a deposition process of a material which can be organic, non-organic, metal, or a mixture of the three materials on a substrate in the form of a plate, thus producing a new property. The application of thin layers for semiconductors is developed in the form of transparent conductive oxide (TCO), sensors, capacitors, diodes, transistors, touch screens, solar cells, and various other forms of technology that are useful for human life today (Imawanti et al., 2017; Paul David et al., 2021).

However, in general, the materials that are often used by researchers in developing thin layers are materials that are included in the metal oxide group. Some examples of these metals include ZnO, SnO₂, and TiO₂. The selection of metal oxides as one of the good materials in the development of thin films is because these materials have the characteristics of high optical transparency at visible light waves and are transparent to light. Various previous studies have proven that the above materials are good precursors in the process of developing various thin layers that have characteristic values according to the needs of various industries, especially those related to electronics. According to Nunes et al. (2002), because of its optical and electrical qualities, high chemical and mechanical stability, and natural availability, ZnO has become one of the most promising materials. ZnO is also used as a base material for thin films because it is readily available, non-toxic, and efficient to produce (Vyas, 2020). The physical properties of ZnO nanostructures: it is important to note that the size of semiconductor materials is continuously decreasing towards the nanometer scale or even smaller, and some of their physical properties undergo changes

known as quantum size effects (Doyan & Humaini, 2017). Understanding the basic physical properties is important for the design of functional devices (Xin et al., 2019).

The next material in the group of oxidation metals that is often used is SnO₂. Of the many constituent elements, titanium (Ti) and zinc (Zn) have the greatest abundance compared to other elements. However, tin (Sn) is a good alternative as a base material for thin layers because it has advantages over other metals, namely it is one of the good electrical conductors with a low electrical resistivity of 4.60 μΩ.cm, easy to form, resistant to corrosion, lightweight, non-flammable, and durable (Doyan et al., 2017, 2021). One of the nanoscale materials, which includes semiconductor materials, is SnO₂. Tin (IV) oxide finds extensive use in sensor gases, solar cells, TCO, and optoelectronic devices (Mulyadi et al., 2019). Furthermore, tin (IV) oxide has a number of benefits, including low resistivity, excellent transparency, good chemical stability, and a band gap width of about 3.6 eV (Schell et al., 2017). Additionally, the tin (IV) oxide is highly sensitive to the atmosphere surrounding it, which makes it useful as a sensor gas (Pandit & Ahmad, 2022).

The last material that is often used in the development of thin films is titanium dioxide. Titanium dioxide, or chemically written as TiO₂, is a semiconductor material with a band gap of 3-4 eV, so it will only absorb light with wavelengths in the ultraviolet color region and is transparent to visible light (Bedghiou et al., 2019; Rizaldi et al., 2022). In addition, physically, titanium dioxide has a low density of 4.23 g/cc, a molecular weight of 79.886 g/mol, a high level of stability, corrosion resistance, a white crystal form, and is acidic, so it does not dissolve in water (Khasanah et al., 2019; Prastiwi et al., 2017).

The three materials above certainly have characteristics that allow them to be used as basic materials or precursors in developing thin films. However, of course, each of these materials still has characteristics that cannot be used optimally in various industries. These characteristics need to be modified in order to adjust the inherent characteristics of each metal material so that it can be used in various technologies. One way that can be done to change the characteristics of the material is by carrying out a doping process (Norris et al., 2008). Some doping that has been used in this study to improve the capabilities of the three precursors above are aluminum, fluorine, indium, and cobalt.

In this study, two methods of thin layer sample preparation processes were used, namely the sol-gel spin coating and dip coating methods. The use of the sol-gel method is certainly due to several advantages, including being able to produce products with low synthesis temperatures, high purity and structural homogeneity, as well as producing electrochemical properties in the form of good conductivity compared to other methods. According to Costa et al. (2025), the sol-gel method allows the manufacture of SiO₂ glass at a relatively lower temperature (~1,000 °C) without significant loss of phosphate because it is immobilized in aluminum-phosphate units. This method allows the preparation of homogeneous aluminophosphosilicate (APS) samples, which cannot be achieved using the melt-quenching

method. Meanwhile, according to Zhang et al. (2025), compared to other methods, powders prepared by the sol-gel method offer advantages such as fine particle size (Najafi, et al., 2022; Sharifi et al., 2023) and easy stoichiometry control (Khalaj et al., 2023). In its implementation, the sol-gel method can be combined with spin coating and dip coating techniques. Both techniques are used by researchers because they have their respective advantages.

Spin coating is a popular and rapid method for coating thin films on substrates. The main advantage of this method is the ease of producing a highly uniform coating. Centripetal force and surface tension of the liquid work together to coat the substrate evenly when a solution of a particular substance is spun at high speed. After excess solvent is removed, spin coating produces a thin film with a thickness ranging from a few nanometers to a few microns (Butt, 2022). The spin coating process is used to coat small materials with diameters ranging from a few square millimeters to a meter or more. One of the main advantages of the spin coating technique is the relative ease and simplicity of the process setup, as well as the thinness and homogeneity (Atay, 2020). Meanwhile, dip coating technique is often used for optical coatings, including wide-area antireflective coatings for sun visors and vehicle rear view mirrors; it is a fast, easy, affordable, and high-quality method used in industrial and laboratory applications (Butt, 2022; Jafri & Jaafar, 2024; Tang & Yan, 2017). During the dip coating process, the substrate is immersed in a solution containing the coating components before the solution is dried (Y. Yang et al., 2018). This method can be described as the deposition of an air-based liquid phase onto the substrate surface.

Research on the synthesis and characterization of thin films has always attracted the attention of scientists because of its wide application in everyday life, both in the fields of decoration, construction, and electronics. In the field of electronics, thin films are used to make semiconductors (Rahmawati & Agustina, 2018). The three precursors used by researchers are certainly expected to have semiconductor material characteristics that are in accordance with several technologies that support human life, such as touch screens, gas sensors, and, of course, solar cells. Solar cell technology is one of the main objectives of thin film development carried out by researchers by applying various precursors and dopant materials to find the best and most efficient characteristic values for the advancement of material research in the future. Based on the problems above, the purpose of this study is to determine and compare the energy band gap values of the precursor materials, namely ZnO, SnO₂, and TiO₂, after being added by various dopants such as zinc, aluminum, fluorine, indium, and cobalt.

METHODS AND MATERIALS

This research is experimental research. This research goes through two main stages, namely the formation of thin layer samples and thin layer characterization tests. The synthesis process itself goes through several stages, including:

- (1) Preparation of research materials, including precursors consisting of zinc acetate dihydrate ($\text{Zn}(\text{CH}_3\text{COO})_2\cdot\text{H}_2\text{O}$), tin (II) chloride dihydrate ($\text{SnCl}_2\cdot 2\text{H}_2\text{O}$), and others, titanium dioxide (TiO_2); solvents consisting of ethanol ($\text{C}_2\text{H}_5\text{OH}$), hydrochloric acid (HCl), and aquades; while the dopant materials used include zinc dichloride (ZnCl_2), aluminum chloride (AlCl_3), indium (III) chloride tetrahydrate ($\text{InCl}_3\cdot 4\text{H}_2\text{O}$), ammonium fluoride (NH_4F), and cobalt (II) chloride ($\text{CoCl}_2\cdot 6\text{H}_2\text{O}$). The media used in the material coating process are glass and quartz substrates.
- (2) Making a sol-gel solution by mixing precursors, solvents, and doping materials into the same container and then stirring using a magnetic stirrer for 30-60 min until the mixture looks homogeneous.
 - (a) ZnO sol-gel solution
 $\text{Zn}(\text{CH}_3\text{COO})_2\cdot 2\text{H}_2\text{O}$ was dissolved into ethanol solution ($\text{C}_2\text{H}_6\text{O}$), and mono ethanolamine (MEA: $\text{C}_2\text{H}_7\text{NO}$) at room temperature with a molar ratio of MEA and ZnAc of 1:1. Then the solution was stirred using a magnetic stirrer at a temperature of $\pm 70^\circ\text{C}$ for 30 min until a homogeneous solution was obtained.
 - (b) SnO_2 sol-gel solution
 $\text{SnCl}_2\cdot 2\text{H}_2\text{O}$ as much as 0.902 g in powder form is dissolved in 40 ml of ethanol. The process of dissolving $\text{SnCl}_2\cdot 2\text{H}_2\text{O}$ in ethanol using a hot plate and stirring using a magnetic stirrer until it reaches a temperature of 80°C for 30 minutes or until the solution is homogeneous. Then dopant materials are added according to the variables used, namely aluminum, indium, and fluorine, and then stirred again until all mixtures look homogeneous.
 - (c) TiO_2 sol-gel solution
 The preparation of TiO_2 sol-gel solution uses 20 ml of ethanol solvent with a fixed concentration of 1 M. After the process of making the precursor solution in the form of TiO_2 , then the addition of NH_4F , Indium(III)Chloride (InCl_3), and cobalt(II)chloride (CoCl_2) doping is carried out according to the mass calculation of each research material. Specifically for the use of CoCl_2 doping, it is necessary to add hydrochloric acid (HCl) solution. This needs to be done so that the CoCl_2 material can be mixed homogeneously with the precursor used.
- (3) The process of depositing sol-gel solution on the substrate, where this stage is the process of coating the substrate material using a previously prepared solution. The deposition process uses aids in the form of a dip coater and a modified centrifuge with the aim that the deposited solution can be evenly distributed over the substrate used (glass or quartz).
- (4) The process of heating thin layer samples using an oven or furnace, which aims to dry and remove other solutions that are still on the surface of the substrate.

In this study, it has been developed into several types of research samples with different treatments. To facilitate the analysis process, the researcher provides categorization or codes (Table 1).

The second stage after the thin film synthesis process is carried out is to conduct a thin film characterization test. In this study, three analysis test processes were carried out, namely 1) using XRD to measure the crystal structure of thin film samples, 2) using a scanning electron microscope (SEM) to determine the morphological structure of the surface of the thin film sample, and 3) using a UV-Vis spectrophotometry tool to determine the distribution of absorbance values of the thin film sample. The data from the UV-Vis spectrophotometry test results were used by researchers to determine the energy band gap value of each thin film sample.

The energy band gap value can be determined using the Tauc plot graphic method, which describes the relationship between $h\nu$ and $(ah\nu)^n$ (Efelina, 2017). The value of $n = \frac{1}{2}$ for the direct energy gap and $n = 2$ for the indirect energy gap (Susilawati et al., 2009). The Tauc determination of the energy band gap from the relationship graph between $h\nu$ and $(ah\nu)^n$ until it intersects the $h\nu$ axis. The method process uses absorbance value data that has been obtained and analyzed using Microsoft Excel 2010. Determination of the energy band gap from the relationship graph between $h\nu$ and $(ah\nu)^n$ until it intersects the $h\nu$ axis. To make it easier to understand the procedure in this study, it can be seen in the following chart (Figure 1).

Table 1
Thin film research samples

No.	Sample	Method	Substrate	Sample code
1	Zinc oxide	Sol-gel dip-coating	Glass	ZnO type A
2	Zinc oxide	Sol-gel spin-coating	Glass	ZnO type B
3	Tin(IV) oxide doping aluminum	Sol-gel spin-coating	Quartz	SnO ₂ :Al type A
4	Tin(IV) oxide doping aluminum	Sol-gel spin-coating	Glass	SnO ₂ :Al type B
5	Tin(IV) oxide doping indium	Sol-gel spin-coating	Glass	SnO ₂ :In
6	Tin(IV) oxide doping fluorine	Sol-gel spin-coating	Glass	SnO ₂ :F
7	Tin(IV) oxide doping aluminum and fluorine	Sol-gel spin-coating	Glass	SnO ₂ :(Al+F)
8	Tin(IV) oxide doping aluminum and indium	Sol-gel spin-coating	Glass	SnO ₂ :(Al+In)
9	Tin(IV) oxide doping aluminum, fluorine, and indium	Sol-gel spin-coating	Glass	SnO ₂ :(Al+F+In)
10	Titanium dioxide doping fluorine and indium	Sol-gel spin-coating	Glass	TiO ₂ :(F+In)
11	Titanium dioxide doping cobalt	Sol-gel spin-coating	Glass	TiO ₂ :Co

Note. ZnO = Zinc oxide; SnO₂:Al = Tin(IV) oxide doped with aluminum; SnO₂:In = Tin(IV) oxide doped with indium; SnO₂:F = Tin(IV) oxide doped fluorine; SnO₂:(Al+F) = Tin(IV) oxide is doped with a mixture of aluminum and fluorine; SnO₂:(Al+In) = Tin(IV) oxide is doped with a mixture of aluminum and indium; SnO₂:(Al+F+In) = Tin(IV) oxide is doped with a mixture of aluminum, fluorine, and indium; TiO₂:(F+In) = Titanium dioxide doped with mixture fluorine and indium; TiO₂:Co = Titanium dioxide doped with cobalt

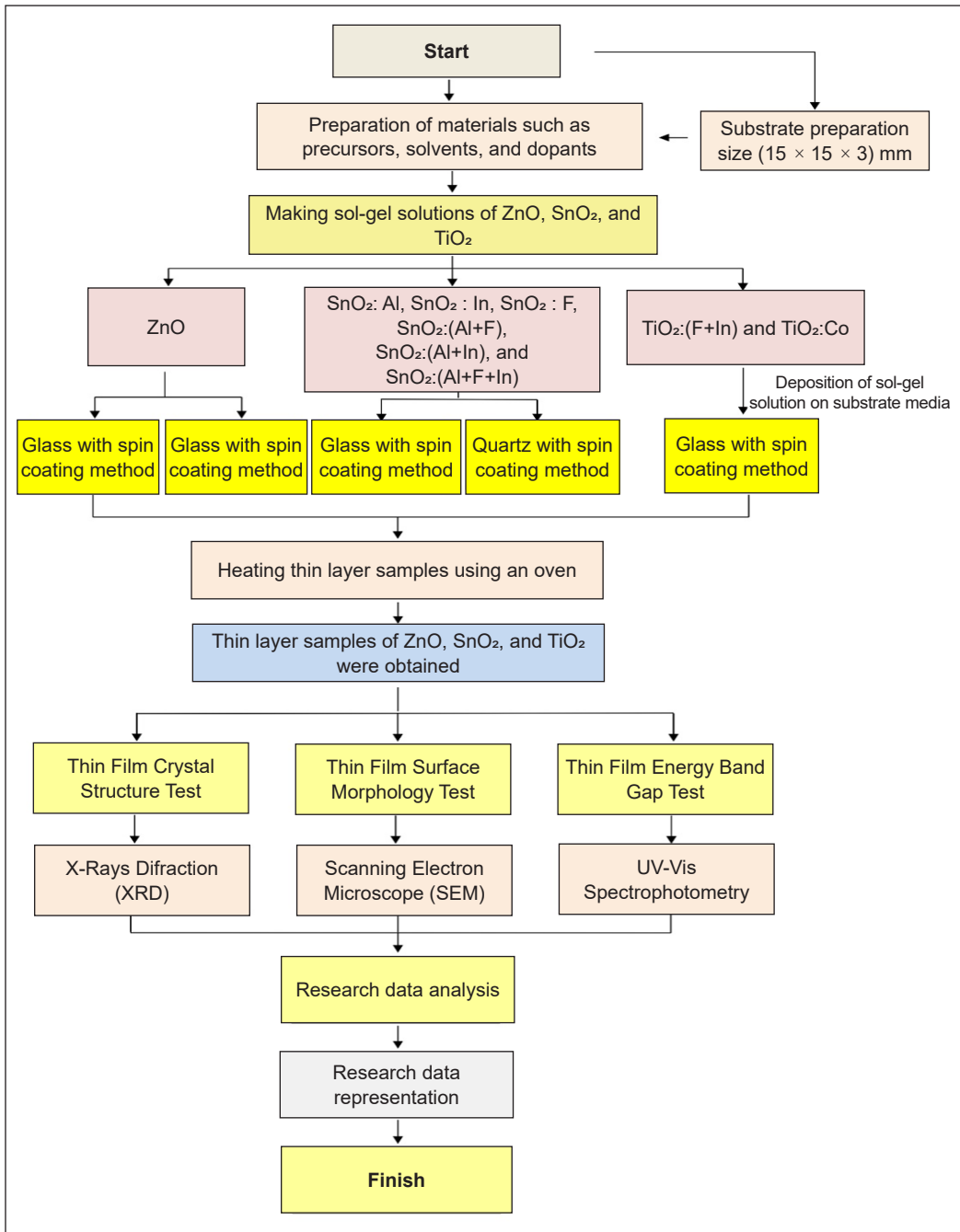


Figure 1. Research stages of ZnO, SnO₂, and TiO₂ thin films

Note. ZnO = Zinc oxide; SnO₂:Al = Tin(IV) oxide doped with aluminum; SnO₂:In = Tin(IV) oxide doped with indium; SnO₂:F = Tin(IV) oxide doped fluorine; SnO₂:(Al+F) = Tin(IV) oxide is doped with a mixture of aluminum and fluorine; SnO₂:(Al+In) = Tin(IV) oxide is doped with a mixture of aluminum and indium; SnO₂:(Al+F+In) = Tin(IV) oxide is doped with a mixture of aluminum, fluorine, and indium; TiO₂:(F+In) = Titanium dioxide doped with mixture fluorine and indium; TiO₂:Co = Titanium dioxide doped with cobalt

RESULTS AND DISCUSSION

Thin Film Synthesis

This study was conducted with the aim of determining the surface morphology structure and energy band gap value of thin films with ZnO, SnO₂, and TiO₂ precursor materials. The process of making thin layer samples begins with the process of determining the mass of each material used in the study, such as precursors and dopants. This is very important to ensure that the mass ratio between precursors and dopants is appropriate so that it can produce a homogeneous solution when mixed. The equation that can be used to determine the total mass of precursors and dopants in the study is as follows.

$$M = \frac{m_t}{m_r} \times \frac{1000}{V} \quad [1]$$

After the total mass of the precursor and dopant materials is obtained, the precursor mass calculation process is carried out according to the concentration used in the study by referring to the following equation.

$$(100 - n)\% = \frac{m_x \text{Prekursor} \times \frac{1}{m_r \text{Prekursor}}}{m_t \text{Dopant} \times \frac{1}{M_r \text{Dopant}}} \quad [2]$$

Where M = molarity; m_t = Total mass of the sample; m_r = Relative molecular mass; V = Volume of solution; n = Concentration; and m_x = Mass of materials used

After carrying out the material calculation process, the solution-making process is carried out by mixing the precursor and dopant with the solvent used. This process aims to ensure that all research materials used can be mixed evenly or homogeneously and produce a sol-gel solution made from ZnO, SnO₂, and TiO₂. The sol-gel solution that has been produced is then subjected to a deposition process using either the dip-coating or spin-coating method on the substrate media. The results of this deposition process are then heated using an oven, and several displays of thin layer samples with ZnO, SnO₂, and TiO₂ precursor materials are obtained as follows in Figure 2.

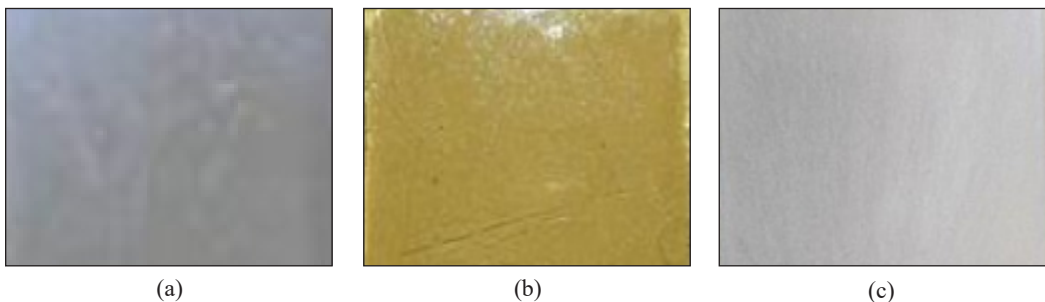


Figure 2. Thin film samples: (a) Zinc oxide, (b) Tin(IV) oxide, and (c) Titanium dioxide

Thin Film Characterization

Characterization is a test process to determine the extent of the character or nature of the research sample that has been carried out. Characterization in this study measures two properties of thin layer samples, namely the surface morphological structure and the energy band gap value.

Thin Film Crystal Structure

The crystal structure of the thin film was tested using XRD data with the aim of determining the crystal orientation phase and crystal size formed in the thin film sample. The measurement uses an angle range of 10° to 90° on the grounds that the crystals will be detected at a diffraction source wavelength of 1.5406 \AA from the CuK α source (Ramesh et al., 2023; X. Yang et al., 2022). The measurement produces data in the form of a diffraction pattern of the relationship between intensity (y-axis) and scattering angle or 2θ (x-axis). Based on the test results, the diffraction pattern of the thin layer sample can be seen in the following Figure 3.

The differences in diffraction patterns are found in thin film samples made from ZnO, SnO₂, and TiO₂ precursors. Of course, each precursor has special characteristics that describe the characteristics of the compound. The diffraction pattern of ZnO crystal planes is (101) and hexagonal ZnO crystal. SnO₂ thin film samples generally have three highest trend peaks, which indicates that the crystal form is tetragonal. This is supported by the results of research conducted by Zaini et al. (2018), which found that the lattice parameters of the synthesized SnO₂ are almost the same as SnO₂ no. COD 969007534 in the form of a

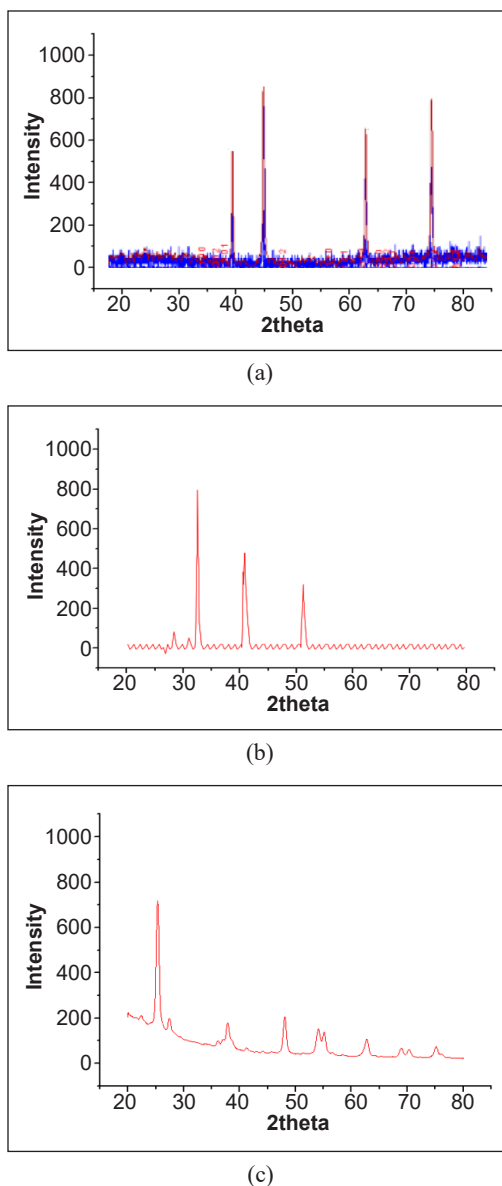


Figure 3. Diffraction patterns of thin film samples: (a) Zinc oxide, (b) Tin(IV) oxide, and (c) Titanium dioxide

tetragonal crystal structure with a space group. Meanwhile, in the TiO₂ sample, it can be seen that the highest intensity is seen, especially in the (101) plane, with the maximum intensity value produced for the highest peak in the TiO₂ sample at the 2θ value of 25°, which is in accordance with the main peak typical of the TiO₂ anatase phase (tetragonal) (Khan et al., 2020; Preeti & Rohilla, 2020). The intensity value obtained from the XRD measurement results illustrates the proportionality to the level of crystallinity of a material, where the higher the intensity of the diffractogram peak, the more perfect the crystal shape formed in the material (Khan et al., 2020; Tjahjanti, 2019).

In addition to determining the phase and form of the crystal structure, XRD test data can be used to determine the crystal grain size of thin film samples. To determine the size of the crystal particles that make up the thin film, it can be calculated by utilizing the XRD test results using the Debye-Scherrer equation (Khan et al., 2020), namely:

$$D = \frac{k\lambda}{\beta \cos\theta} \quad [3]$$

Where D = Crystal size; k = Material constant (usually 0.9); θ = Diffraction angle; λ = The wavelength of the X-ray source used; and β = Full width at half maximum (FWHM) value

Based on the results of the crystal size calculations obtained in the ZnO, SnO₂, and TiO₂ samples, they can be seen in Table 2.

Based on Table 2, it can be seen that the thin film sample with ZnO material has the smallest crystal grain size compared to the other two precursors. The width of the XRD spectrum, specifically the FWHM value, influences the value of the crystal grain size. If the FWHM value is small, the crystal grain size is large, and vice versa. Data related to crystal grain size can be used as an indicator to explain the catalytic ability of a thin film, where the smaller the crystal grain size, the larger the particle surface area so that the catalytic power will be better (Putra Parmita et al., 2023; Xian et al., 2019). According to research conducted by Li et al. (2020), photocatalysts with nano sizes ranging from 1 to 100 nm will provide high catalytic activity.

Table 2
Comparison of crystal grain size of thin film samples

Sample	Scattering angle (2θ) (deg)	Miller index (hkl)	FWHM (deg)	Crystalline grain size (D) (nm)
ZnO	44.48	101	0.2086	14.45
SnO ₂	26.60	110	0.0028	43.43
TiO ₂	27.44	101	0.1882	15.16

Note. ZnO = Zinc oxide; SnO₂ = Tin(IV) oxide; TiO₂ = Titanium dioxide; FWHM = Full width at half maximum

Thin Layer Surface Morphology Structure

The morphological structure of the layer can be seen using a SEM. The test method with this tool uses a high-energy beam of electrons to scan the object to produce an image and sample composition (Sahdiah & Kurniawan, 2023). The images produced by this method have better resolution and image detail than an optical microscope because the electron beam used as a source has a wavelength tens of thousands of times shorter than the wavelength of light.

The three precursors used illustrate that the surface appearance of the TiO₂ thin film has a more regular and symmetrical distribution when compared to other materials, as seen in Figure 4. Each material has its own characteristics; this can be seen in that the ZnO precursor has an appearance like a root distribution along the surface of the thin layer. This is in line with the results of research conducted by Ridhuan et al. (2012), which showed that the agglomeration process still occurs, causing the surface morphology of the particles to be larger and in the form of nanorods. This is possible because the calcination process is not yet perfect so that there is still a part of the extract that coats the particles. However, if referring to its performance, the surface conditions of this ZnO have quite high potential related to the energy band gap value. Due to lower grain boundaries, surface defects, interference, and discontinuous interfaces, one-dimensional ZnO nanostructures, such as nanorods, nanowires, and nanotubes, allow for more efficient carrier transport (Chowdhury & Bhowmik, 2021; Dutta et al., 2023).

The morphology of the sample using SnO₂ looks almost even, but there are still many cracks or boundaries along the surface of the thin layer. These cracks indicate that the deposition process of the SnO₂ solution on the substrate media is still not evenly distributed so that when the sample goes through the heating process, there is a part of the substrate surface that is only coated by the solvent used. When the heating process is carried out, of course the goal is to remove the solvent that is still present during the deposition process so that there are parts of the thin layer surface that do not contain SnO₂. To find out more specifically the inner structure of the thin layer with ZnO, SnO₂, and TiO₂ precursors, an

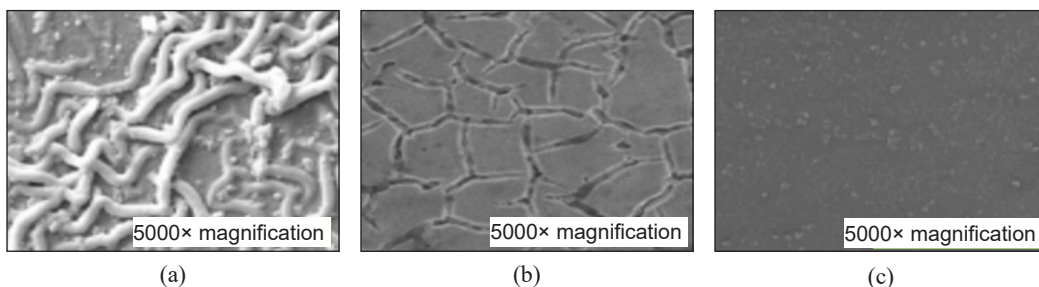


Figure 4. Morphological structure of surface part of thin film with precursors at 5,000× magnification : (a) Zinc oxide, (b) Tin(IV) oxide, and (c) Titanium dioxide

observation enlargement process is carried out so that researchers can watch in detail the inside of the sample, as seen in Figure 5.

TiO₂ thin film sample has a denser structure compared to the ZnO and SnO₂ samples. The size of the constituent particles also looks almost the same, namely in the form of round particles that have denser cavities, indicating that the distribution of the sol-gel solution is evenly distributed throughout the surface of the substrate used. There is agglomeration between neighboring particles, so that the particle size increases again due to the merging of neighboring particles. The shape of the TiO₂ sample particles tends to resemble balls, where the particle size is large and agglomeration occurs in the sample (Listanti et al., 2018). This condition allows the formation of denser crystal particles and increases the ability of TiO₂ in the absorption process. This is what makes TiO₂ one of the precursors that is often used in developing solar cell nanoparticle technology.

In the three results, it can be seen that SnO₂ and TiO₂ have almost the same crystal structure. Both precursors have a round shape that forms the surface of the thin film. This is supported by the results of research conducted by Firooz et al. (2009), where in their research one of the forms of the structure of the thin layer made from SnO₂ is granules apart from the flower and sheet forms. This is different from ZnO, which has a structure resembling a tube or is often called nanorods. The nanostructures of ZnO are very diverse, such as nanobelts, nanoplatelets, nanowires, and nanorods (Novitasari et al., 2022; Raub et al., 2024).

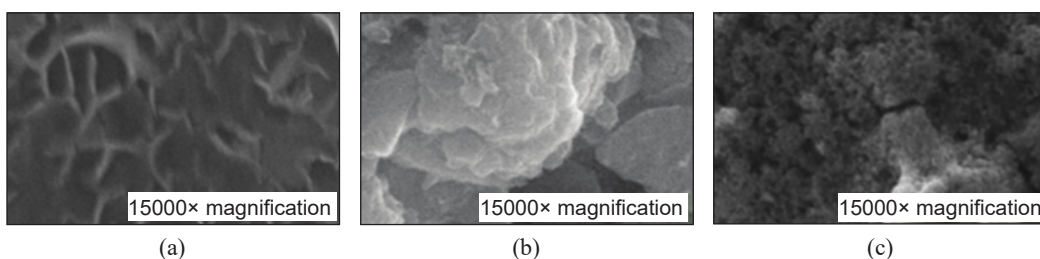


Figure 5. Morphological form of the inner structure of thin layers with precursors at 15,000× magnification: (a) Zinc oxide, (b) Tin(IV) oxide, and (c) Titanium dioxide

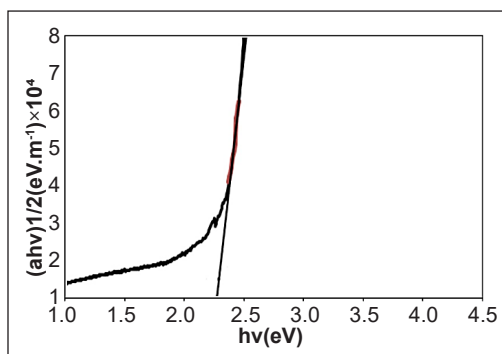
Thin Film Energy Band Gap

The energy band gap is the most important part or one of the indicators that need to be considered in the development process of various nanoparticle technologies. The energy band gap value describes the ability of a material to conduct electricity (Bouzidi et al., 2024). So that good materials in thin film technology must be able to enter the semiconductor material category. Semiconductors are materials that have electrical conductivity between conductors and insulators, or materials that have resistivity between conductors and insulators, namely 10^{-2} - $10^9 \Omega\text{m}$ (Maslakah, 2015). In semiconductor materials, the valence

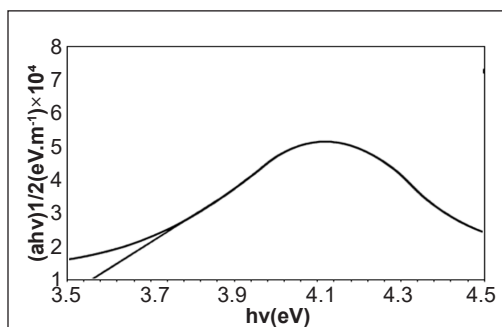
band condition is almost full, and the conduction band is almost empty with a very small forbidden band width (E_g) (± 1 to 2 eV) (Tjahjanti, 2019; Woods-Robinson et al., 2020). It is necessary to know the measurement of the energy band gap of a semiconductor material because the nature of the energy band gap has implications for the differences in the nature of the dependence of the absorbance coefficient on the photon frequency (Mikrajudin, 2010, as cited in Doyan & Humaini, 2017, p. 38). The process of calculating the energy band gap using the absorption value data of the thin layer sample analyzed using the Tauc Plot approach to obtain a slope that describes the relationship between $(ah\nu)^n$ and photon energy ($h\nu$). The Tauc Plot graph that represents the energy band gap value of the thin layer sample can be seen in the following image.

The energy band gap value in each thin layer can be determined by extrapolating from the relationship graph ($h\nu$) as the abscissa and $(ah\nu)^n$ as the ordinate until it intersects the energy axis (the resulting slope graph) and the optical band gap value is obtained. Of course, by using this approach, we obtain energy band gap values that are easier to represent, as seen in Figure 6. By using the same approach and method, then in this study, there are at least 11 research samples derived from three precursor materials, namely ZnO, SnO₂, and TiO₂, and using 4 dopant materials, namely indium (In), aluminum (Al), fluorine (F), and cobalt (Co). To facilitate the discussion process, all samples and the energy band gap value for each thin film sample in this study have been recorded (Table 3).

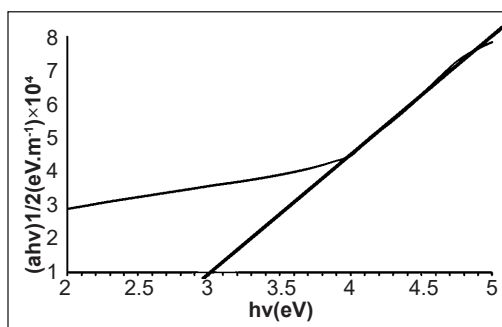
To analyse in depth the various factors that affect the energy band gap value, the use of the solution deposition method, the use of substrates, and the influence of dopants can be seen in the following description.



(a)



(b)



(c)

Figure 6. Comparison of Tauc Plot graphs of energy band gap of thin films: (a) Zinc oxide, (b) Tin(IV) oxide, and (c) Titanium dioxide

Table 3
Thin film energy band gap

No.	Sample	Sample code	Energy band gap value (eV)
1	Zinc oxide	ZnO type A	2.00 – 2.10
2	Zinc oxide	ZnO type B	2.03 – 2.98
3	Tin(IV) oxide doping aluminum	SnO ₂ :Al type A	3.24 – 3.30
4	Tin(IV) oxide doping aluminum	SnO ₂ :Al type B	3.50 – 3.57
5	Tin(IV) oxide doping indium	SnO ₂ :In	3.55 – 3.62
6	Tin(IV) oxide doping fluorine	SnO ₂ :F	3.53 – 3.59
7	Tin(IV) oxide doping aluminum and fluorine	SnO ₂ :(Al+F)	3.47 – 3.56
8	Tin(IV) oxide doping aluminum and indium	SnO ₂ :(Al+In)	3.45 – 3.51
9	Tin(IV) oxide doping aluminum, fluorine, and indium	SnO ₂ :(Al+F+In)	3.36 – 3.50
10	Titanium dioxide doping fluorine and indium	TiO ₂ :(F+In)	2.97 – 3.23
11	Titanium dioxide doping cobalt	TiO ₂ :Co	3.22 – 3.44

Note. ZnO = Zinc oxide; SnO₂:Al = Tin(IV) oxide doped with aluminum; SnO₂:In = Tin(IV) oxide doped with indium; SnO₂:F = Tin(IV) oxide doped fluorine; SnO₂:(Al+F) = Tin(IV) oxide is doped with a mixture of aluminum and fluorine; SnO₂:(Al+In) = Tin(IV) oxide is doped with a mixture of aluminum and indium; SnO₂:(Al+F+In) = Tin(IV) oxide is doped with a mixture of aluminum, fluorine, and indium; TiO₂:(F+In) = Titanium dioxide doped with mixture fluorine and indium; TiO₂:Co = Titanium dioxide doped with cobalt

The Effect of Using Prekursor

Referring to the energy band gap value in Table 3, it can be seen that the ZnO thin film has the smallest energy band gap value compared to other thin film samples using SnO₂ and TiO₂ precursor materials. Both ZnO thin film samples using the dip-coating and spin-coating methods have the lowest energy band gap, reaching a value of 2.00. This condition certainly allows for easy electron transfer from the valence band to the conduction band. If the width of the energy gap decreases, it allows more electrons to undergo electronic transitions from the valence band to the conduction band so that the thin film becomes more conductive (Klein et al., 2010).

In general conditions, ZnO already has an energy band gap value of 3.37 eV and a binding energy of 60 MeV (Tarwal & Patil, 2011). ZnO and TiO₂ are two types of materials that have good energy band gap values in the process of developing solar cell technology when compared to SnO₂. In optimizing the efficiency of perovskite solar cells, one of the materials that plays an important role is the electron transport material (electron transport material [ETM]) made of metal oxide semiconductors such as TiO₂ and ZnO (Yurestira et al., 2021).

In addition to its energy band gap value, ZnO is considered a basic material for the development of various nanoparticle technologies because this material can be developed using various methods, not only focusing on dip-coating and spin-coating.

ZnO nanomaterials can be synthesized using several methods, including vapor-liquid-solid (VLS), aqueous chemical growth (ACG), chemical vapor deposition (CVD), electrochemical deposition (ECD), physical vapor deposition (PVD), metal-organic chemical vapor deposition (MOCVD), and chemical vapor transport and condensation (CVTC) (Maddu et al., 2023; Santibenchakul et al., 2018; Silva et al., 2022; Veerabhadraiah et al., 2022).

Referring to the size of the crystal structure of each precursor component as seen in Table 2, the smaller the energy band gap value produced, the smaller the crystal grain size value. ZnO with the smallest crystal size has an average energy band gap value lower than the precursors SnO₂ and TiO₂. Of the three precursors, it can be seen that ZnO and TiO₂ tend to have the same energy band gap crystal grain size. This is because both materials have almost the same physical and chemical properties as precursor materials in the development of thin film research. In other studies, it was found that these two precursors can be used as materials that are paired and formed into multi-layers (Bhatti et al., 2019; Boukerche et al., 2019; Rad et al., 2023). According to Hakim and Haris (2016), small crystal sizes can expand the catalyst surface so that the catalyst performance becomes more effective, which indicates that the energy band gap value will also decrease, thus increasing the catalyst performance in thin layers.

The Effect of Using the Solution Deposition Method

In this study, to see the extent to which the use of variations in solution deposition methods differs, two methods most often used by researchers are used, namely, dip-coating and spin-coating. The use of these two methods can be seen in thin layers of ZnO precursor material with sample codes ZnO type A for the sol-gel dip-coating method and ZnO type B for the sol-gel spin-coating method. Based on the data in Table 3, it can be seen that the two ZnO samples have energy band gap values that are not much different. The ZnO sample with the dip coating method has a lower energy band gap value with the smallest value at 2.00 eV and the highest at 2.10 eV. A comparison of the lowest and highest energy band gap values between the two samples can be seen in Figure 7.

The energy band gap value in the thin film sample has a significant difference at the highest value. Referring to the results

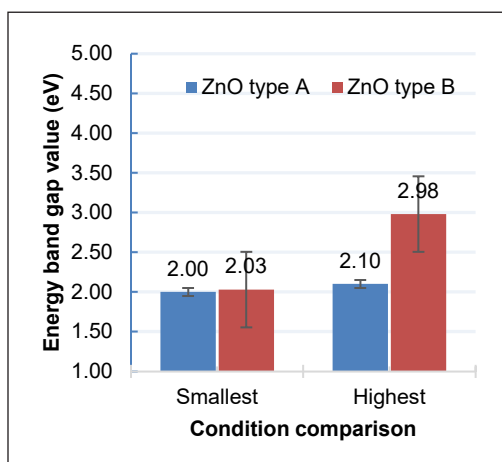


Figure 7. Comparison of energy band gap values of zinc oxide (ZnO) thin films based on the layer deposition method

above, the ZnO type A thin film has a much better value because the range of its values is in the range of 2.00 - 2.10 eV, while in the ZnO type B thin film sample, the range of energy band gap values is 2.03 - 2.98 eV. In thin film development research, the slightest difference in the energy band gap value greatly affects the performance of the device. The use of the dip-coating method provides better energy band gap values compared to using the spin-coating method.

The dip-coating method is a process where a substrate is dipped into a solution and then lifted vertically at a constant speed (Tang & Yan, 2017). The precursor solution that sticks to the substrate and forms a thin layer because the solvent will evaporate and some of the solution will fall due to gravity (Brinker, 2013). The thickness of the solution can be adjusted according to the speed of the substrate withdrawal. This method has been successfully used to create a thin layer of ferroelectric and electronic semiconductor materials (Mukhsinin et al., 2019). This method is widely in demand because the process is simple and does not require expensive costs; besides, it does not damage the environment, and the equipment used is not so complex (Djarwanti & Syahrono, 2014; Patil et al., 2023).

The Effect of Using Substrate Media

The substrate media used in this study consisted of two types, namely glass and quartz. Both of these materials generally have almost the same characteristics because they are included in TCO materials; only for quartz, it is composed of minerals formed from silicon and oxygen chemical compounds with the chemical composition SiO_2 (Imawanti et al., 2017). The selection of media use needs to be considered by researchers; the orientation of the substrate material affects the characteristics of nucleation and growth that dominate the microstructural properties and physical properties of thin films (Mousa et al., 2015).

To determine the effect of using substrate media in this study, we refer to the sample code SnO_2 :Al type A using quartz media and the sample code SnO_2 :Al type B using glass media as seen in Figure 8. The difference in energy band gap values in the two types of media can be seen in the following graph.

The SnO_2 type A thin film sample using quartz as a substrate produces a smaller energy band gap value compared to using glass. This difference is seen both in the smallest and largest values. This certainly

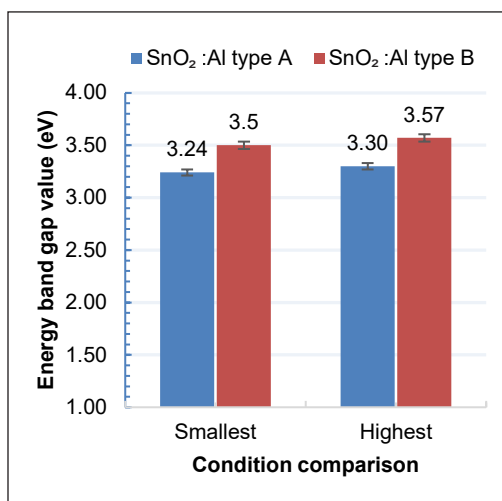


Figure 8. Comparison of energy band gap values of tin(IV) oxide (SnO_2) thin films based on substrate media

indicates that the use of media has an effect on the energy band gap value produced in the thin film sample. An important difference between quartz glass and ordinary glass is its good transmittance across the spectrum, especially in the ultraviolet and deep ultraviolet spectra, which are not available in ordinary optical glass (Ehrt, 2018; Khashan & Nassif, 2001).

Quartz is the most important polymorph of the silica group (SiO_2) and one of the purest minerals in the earth's crust. The SiO_2 system is quite intricate. Despite having the straightforward chemical formula SiO_2 , it has at least 15 known variations or polymorphs, or mineral phases with distinct crystal shapes but the identical stoichiometric composition (Götze et al., 2021). As a major component of sedimentary, metamorphic, and magmatic rocks, quartz is the most significant silica polymorph found in nature. Furthermore, one silica raw material that is economically significant is quartz. Single crystals and polycrystalline quartz are both utilized in industry, for instance, as silicon metal ore, refractory materials, or high-purity quartz crystals or sands (Götze et al., 2021).

The Effect of Using Dopant

Doping is a process that aims to change the characteristics of a material so that it can achieve certain conditions and according to the needs required by researchers. The use of various dopants is certainly one of the alternative variables that are often used by researchers to determine the extent of the properties produced in thin layers. In this study, of course, the main purpose of using dopant variations is to obtain thin layer samples with the smallest energy band gap values. Research data related to the effect of dopant use can be observed in samples with SnO_2 and TiO_2 precursor materials, where both precursors are treated with cross-sections of various types of dopants such as aluminum, indium, fluorine, and cobalt. Data related to the comparison of energy band gap values in thin layers made of SnO_2 and TiO_2 (Figures 9 and 10).

The dopant incorporation process gives a better effect on the process of reducing the energy band gap in both SnO_2 and TiO_2 precursors. This can be seen from the results of the values of each sample, namely SnO_2 : (Al+ F+In) and TiO_2 : (F+In), which have the smallest energy band gap values with values of 3.36 and 2.97 eV, respectively. If researchers look at the overall results of the energy band gap values of thin film samples, it can be seen that the use of various dopants gives varying results. This is certainly because the characteristics of each element are different from one another.

Various studies have shown that the use of two or more dopants in one deposition process has a better impact on changing the properties or characteristics of thin film samples. Research conducted by Han et al. (2018) proved that tridoping has higher photocatalytic activity compared to pure SnO_2 , SnO_2 -ZnO, or mono- or di-doped SnO_2 -ZnO thin films. SnO_2 -ZnO tridoped B/Ag/F composite thin films have the highest photocatalytic

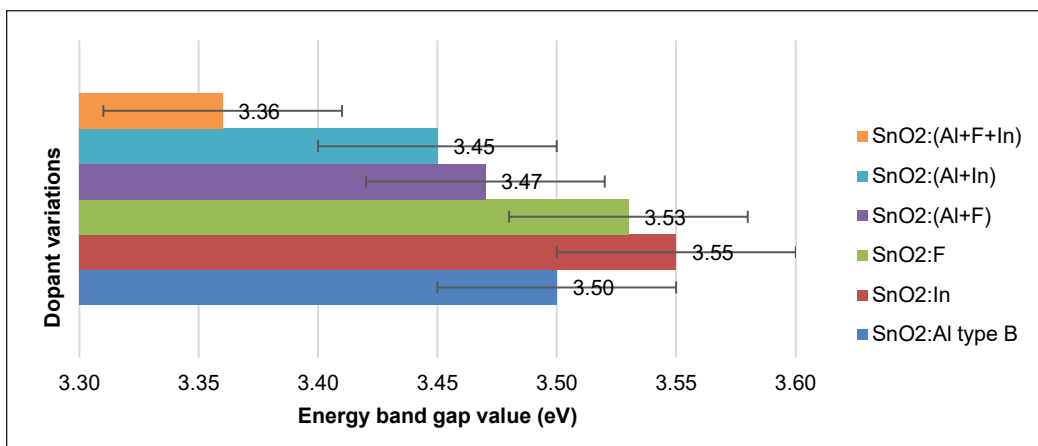


Figure 9. Comparison of Tin(IV) oxide (SnO₂) energy band gap values based on dopant variables
 Note. SnO₂:(Al+F+In) = Tin(IV) oxide is doped with a mixture of aluminum, fluorine, and indium; SnO₂:(Al+In) = Tin(IV) oxide is doped with a mixture of aluminum and indium; SnO₂:(Al+F) = Tin(IV) oxide is doped with a mixture of aluminum and fluorine; SnO₂:F = Tin(IV) oxide doped fluorine; SnO₂:In = Tin(IV) oxide doped with indium; SnO₂:Al = Tin(IV) oxide doped with aluminum

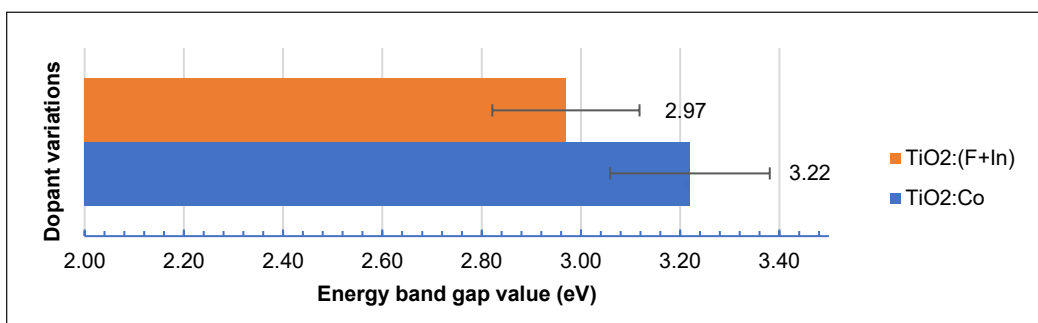


Figure 10. Comparison of Titanium dioxide (TiO₂) energy band gap values based on dopant variables
 Note. TiO₂:(F+In) = Titanium dioxide doped with mixture fluorine and indium; TiO₂:Co = Titanium dioxide doped with cobalt

activity. The composition of SnO₂-ZnO and tridoping B/Ag/F are very important for the photocatalytic activity of thin films. The low electron-hole pair recombination rate and strong light absorption appear to be correlated with the increased activity of SnO₂-ZnO tridoped B/Ag/F thin films.

The same condition also occurs in the thin layer of TiO₂ that the provision of double doping is able to produce better characteristics compared to the use of single doping. This is supported by research conducted by Ashkarran et al. (2014), which obtained the results that after optimizing the dopant concentration, the research findings showed that TiO₂ nanoparticles (NPs) with double doping had the highest photocatalytic and antibacterial activities when compared to TiO₂ NPs with single doping. In contrast, TiO₂ NPs with silver

and nitrogen doping expanded the light absorption spectrum towards the visible region and significantly increased the photodegradation of model dyes and inactivation of bacteria under visible light irradiation. When TiO₂ is exposed to visible light, two different electronic states capture its inner electrons and narrow the band gap. This changes the optical response from the ultraviolet region to the visible light region, which is responsible for the better photocatalytic activity and antibacterial quality of TiO₂ NPs with double doping.

CONCLUSION

Based on the results of data analysis and discussion, it can be concluded that 1) the crystal structure of ZnO thin films is hexagonal while SnO₂ and TiO₂ are tetragonal, 2) the surface morphology of SnO₂ and TiO₂ thin films is granular, while ZnO thin films are nanorod, and 3) the smallest energy band gap value is found in ZnO thin films with a value of 2.00 eV. There are four factors that affect the energy band gap value in thin films, namely precursor materials, deposition methods, substrate media, and dopant materials. Each variable that produces the smallest energy band gap value in this study is the ZnO precursor, dip-coating method, quartz substrate media, and the use of double or triple dopants in one deposition treatment.

ACKNOWLEDGEMENTS

The author would like to thank those who have helped in making this article, especially the Laboratory Analytical Chemistry and Basic Chemistry Laboratory of the Faculty of Mathematics and Natural Sciences at Mataram University, the Integrated Science Laboratory of Mataram State Islamic University, the Laboratory Physics Department Institute Technology Bandung, and the Integrated Laboratory of Diponegoro University.

REFERENCES

- Ashkarran, A. A., Hamidinezhad, H., Haddadi, H., & Mahmoudi, M. (2014). Double-doped TiO₂ nanoparticles as an efficient visible-light-active photocatalyst and antibacterial agent under solar simulated light. *Applied Surface Science*, 301, 338-345. <https://doi.org/10.1016/j.apsusc.2014.02.074>
- Atay, H. Y. (2020). Fabrication methods for polymer coatings. In Inamuddin., R. Boddula, M. I. Ahamed, & A. M. Asiri (Eds.), *Polymer coatings: Technology and applications* (pp. 1-20). Scrivener Publishing. <https://doi.org/10.1002/9781119655145.ch1>
- Bedghiou, D., Reguig, F. H., & Boumaza, A. (2019). Novel high/ultrahigh pressure structures of TiO₂ with low band gaps. *Computational Materials Science*, 166, 303-310. <https://doi.org/10.1016/j.commatsci.2019.05.016>
- Bhatti, K. A., Khan, M. I., Saleem, M., Alvi, F., Raza, R., & Rehman, S. (2019). Analysis of multilayer based TiO₂ and ZnO photoanodes for dye-sensitized solar cells. In *Materials Research Express* (Vol. 6, No. 7, p. 075902). IOP Publishing. <https://doi.org/10.1088/2053-1591/ab11e8>

- Boukerche, S., Himour, A., Bououdina, M., Bensouici, F., & Ouchenane, S. (2019). Multilayered ZnO/TiO₂ nanostructures as efficient corrosion protection for stainless steel 304. In *Materials Research Express* (Vol. 6, No. 5, p. 055052). IOP Publishing. <https://doi.org/10.1088/2053-1591/ab042f>
- Bouzidi, M., Bechir, M. B., Almalawi, D. R., Smaili, I. H., & Aljuaid, F. (2024). From molecular salt to layered network: cation-driven tuning of band gap, structure, and charge transport in A₃Bi₂I₉ (A= Cs, Rb) perovskites. *RSC Advances*, 14(32), 23058-23072. <https://doi.org/10.1039/D4RA04464A>
- Brinker, C. J. (2013). Dip coating. In T. Schneller, R. Waser, M. Kosec, & D. Payne (Eds.), *Chemical solution deposition of functional oxide thin films* (pp. 233-261). Springer. https://doi.org/10.1007/978-3-211-99311-8_10
- Butt, M. A. (2022). Thin-film coating methods: A successful marriage of high-quality and cost-effectiveness - A brief exploration. *Coatings*, 12(8), 1115. <https://doi.org/10.3390/coatings12081115>
- Chowdhury, N. K., & Bhowmik, B. (2021). Micro/nanostructured gas sensors: The physics behind the nanostructure growth, sensing and selectivity mechanisms. *Nanoscale Advances*, 3(1), 73-93. <https://doi.org/10.1039/D0NA00552E>
- Costa, B. H., Tayama, G. T., Rivera, V. A. G., Messaddeq, Y., & Santagneli, S. H. (2025). Effects of the thermal treatment on structural and luminescence properties of Er³⁺-doped aluminophosphosilicate glasses obtained by the sol-gel method. *Journal of Alloys and Compounds*, 1010, 177112. <https://doi.org/10.1016/j.jallcom.2024.177112>
- Djarwanti, D., & Syahroni, C. (2014). Pengaruh H₂O₂, pH dan sumber sinar pada degradasi air limbah pewarna indigo menggunakan katalis TiO₂ [Influence of H₂O₂, pH, and light source on the degradation of indigo dye wastewater using TiO₂ catalyst]. *Jurnal Riset Teknologi Pencegahan Pencemaran Industri*, 5(1), 7-14. <https://doi.org/10.21771/jrtpi.2014.v5.no1.p7-14>
- Doyan, A., & Humaini, H. (2017). Sifat optik lapisan tipis ZnO [Optical properties of ZnO thin layers]. *Jurnal Pendidikan Fisika dan Teknologi*, 3(1), 34-39. <https://doi.org/10.29303/jpft.v3i1.321>
- Doyan, A., Susilawati, & Imawanti, Y. D. (2017). Synthesis and characterization of SnO₂ thin layer with a doping aluminum is deposited on quartz substrates. In *AIP Conference Proceedings* (Vol. 1801, No. 1, p. 020005). AIP Publishing. <https://doi.org/10.1063/1.4973083>
- Doyan, A., Susilawati, & Munandar, H. (2021). Optical characteristics of tin oxide thin films doped with indium and aluminum using the sol-gel spin coating technique. In *Proceedings of the 7th International Conference on Research, Implementation, and Education of Mathematics and Sciences* (pp. 396-403). Atlantis Press. <https://doi.org/10.2991/assehr.k.210305.057>
- Dutta, T., Noushin, T., Tabassum, S., & Mishra, S. K. (2023). Road map of semiconductor metal-oxide-based sensors: A review. *Sensors*, 23(15), 6849. <https://doi.org/10.3390/s23156849>
- Efelina, V. (2017). Preparasi dan penentuan energi gap film tipis TiO₂:Cu yang ditumbuhkan menggunakan spin coating [Preparation and determination of gap energy of TiO₂:Cu thin films grown using spin coating]. *Jurnal Pendidikan Fisikadan Keilmuan*, 3(1), 19-27. <https://doi.org/10.25273/jpfk.v3i1.941>

- Ehrt, D. (2018). Deep-UV materials. *Advanced Optical Technologies*, 7(4), 225-242. <https://doi.org/10.1515/aot-2018-0023>
- Firooz, A. A., Mahjoub, A. R., & Khodadadi, A. A. (2009). Effects of flower-like, sheet-like and granular SnO₂ nanostructures prepared by solid-state reactions on CO sensing. *Materials Chemistry and Physics*, 115(1), 196-199. <https://doi.org/10.1016/j.matchemphys.2008.11.028>
- Götze, J., Pan, Y., & Müller, A. (2021). Mineralogy and mineral chemistry of quartz: A review. *Mineralogical Magazine*, 85(5), 639-664. <https://doi.org/10.1180/mgm.2021.72>
- Hakim, A. R., & Haris, A. (2016). Sintesis fotokatalis ZnO-Al dan aplikasinya pada degradasi fenol dan reduksi Cd(II) secara simultan [Synthesis of ZnO-Al photocatalyst and its application in simultaneous phenol degradation and Cd(II) reduction]. *Jurnal Kimia Sains dan Aplikasi*, 19(1), 7-10. <https://doi.org/10.14710/jksa.19.1.7-10>
- Han, K., Peng, X.-L., Li, F., & Yao, M.-M. (2018). SnO₂ composite films for enhanced photocatalytic activities. *Catalysts*, 8(10), 453. <https://doi.org/10.3390/catal8100453>
- Imawanti, Y. D., Doyan, A., & Gunawan, E. R. (2017). Sintesis lapisan tipis (thin film) SnO₂ dan SnO₂: Al menggunakan teknik sol-gel spin coating pada substrat kaca dan quartz [Thin film synthesis of SnO₂ and SnO₂: Al using sol-gel spin coating techniques on glass and quartz substrates]. *Jurnal Penelitian Pendidikan IPA*, 3(1). <https://doi.org/10.29303/jppipa.v3i1.49>
- Jafri, N. N. M., & Jaafar, J. (2024). Dip coating technique. In M. H. D. Othman, M. A. Rahman, T. Matsuura, M. R. Adam, & S. N. N. M. Makhtar (Eds.), *Advanced ceramics for photocatalytic membranes* (pp. 101-127). Elsevier. <https://doi.org/10.1016/B978-0-323-95418-1.00016-1>
- Khalaj, G., Soleymani, F., Sharifi, F., & Najafi, A. (2023). Evaluation of APC impact on controlling precursors properties in the sol for synthesizing meso porous ZrC nanopowder through sol-gel process. *Journal of Materials Research and Technology*, 26, 6182-6192. <https://doi.org/10.1016/j.jmrt.2023.08.287>
- Khan, H., Yerramilli, A. S., D'Oliveira, A., Alford, T. L., Boffito, D. C., & Patience, G. S. (2020). Experimental methods in chemical engineering: X-ray diffraction spectroscopy - XRD. *The Canadian Journal of Chemical Engineering*, 98(6), 1255-1266. <https://doi.org/10.1002/cjce.23747>
- Khasanah, J. U., Mukaromah, A. H., & Dewi, S. S. (2019). Penurunan jumlah bakteri *Eschercherichia coli* dengan penyaringan membran zeolit ZSM-5/TiO₂ [Decreasing the number of *Eschercherichia coli* bacteria by ZSM-5/TiO₂ zeolite membrane filtering]. *Prosiding Seminar Nasional Mahasiswa Unimus*, 2, 271-276.
- Khashan, M. A., & Nassif, A. Y. (2001). Dispersion of the optical constants of quartz and polymethyl methacrylate glasses in a wide spectral range: 0.2–3 μm. *Optics Communications*, 188(1-4), 129-139. [https://doi.org/10.1016/S0030-4018\(00\)01152-4](https://doi.org/10.1016/S0030-4018(00)01152-4)
- Klein, A., Körber, C., Wachau, A., Säuberlich, F., Gassenbauer, Y., Harvey, S. P., Harvey, S. P., Proffit, D. E., & Mason, T. O. (2010). Transparent conducting oxides for photovoltaics: Manipulation of fermi level, work function and energy band alignment. *Materials*, 3(11), 4892-4914. <https://doi.org/10.3390/ma3114892>
- Koziej, D., Lauria, A., & Niederberger, M. (2014). 25th anniversary article: Metal oxide particles in materials science: Addressing all length scales. *Advanced Materials*, 26(2), 235-257. <https://doi.org/10.1002/adma.201303161>

- Li, D., Song, H., Meng, X., Shen, T., Sun, J., Han, W., & Wang, X. (2020). Effects of particle size on the structure and photocatalytic performance by alkali-treated TiO₂. *Nanomaterials*, *10*(3), 546. <https://doi.org/10.3390/nano10030546>
- Listanti, A., Taufiq, A., Hidayat, A., & Sunaryono, S. (2018). Investigasi struktur dan energi band gap partikel nano TiO₂ hasil sintesis menggunakan metode sol-gel [Investigation of the structure and band gap energy of TiO₂ nanoparticles synthesized using the sol-gel method]. *Journal of Physical Science and Engineering*, *3*(1), 8-15. <https://doi.org/10.17977/um024v3i12018p008>
- Maddu, A., Zikri, Z., & Irzaman, I. (2023). Structure and morphology of ZnO nanoparticles prepared by sonochemical method. *TIME in Physics*, *1*(2), 51-58. <https://doi.org/10.11594/timeinphys.2023.v1i2p51-58>
- Maslakah, U. (2015). *Analisis lebar celah pita energi dan ikatan molekul lapisan tipis a-Si:H yang ditumbuhkan dengan metode PECVD* [Analysis of energy band gap and molecular bonding of a-Si:H thin films deposited by PECVD method] [Bachelor's thesis, Institut Teknologi Sepuluh Nopember]. ITS Repository. <https://repository.its.ac.id/51894/1/1110100030-Undergraduate%20Thesis.pdf>
- McIvor, R., & Humphreys, P. (2004). Early supplier involvement in the design process: Lessons from the electronics industry. *Omega*, *32*(3), 179-199. <https://doi.org/10.1016/j.omega.2003.09.005>
- Mousa, A. O., Habubi, N. F., & Nema, N. A. (2015). Substrate effects on structural and optical properties of ZnO thin films deposited by chemical spray pyrolysis. *International Letters of Chemistry, Physics and Astronomy*, *51*, 69-77. <https://doi.org/10.56431/p-gcf022>
- Mukhsinin, A., Nehru, N., & Afrianto, M. F. (2019). Rancang bangun alat pembuat lapisan tipis metode dip coating berbasis arduino uno [Design and build a thin layer maker using the arduino uno based dip coating method]. *Jurnal Ilmu Fisika dan Pembelajarannya*, *3*(2), 76-83. <https://doi.org/10.19109/jifp.v3i2.4117>
- Muliyadi, L., Doyan, A., Susilawati, S., & Hakim, S. (2019). Synthesis of SnO₂ thin layer with a doping fluorine by sol-gel spin coating method. *Jurnal Penelitian Pendidikan IPA*, *5*(2), 175-178. <https://doi.org/10.29303/jppipa.v5i2.257>
- Najafi, A., Sharifi, F., Mesgari-Abbasi, S., & Khalaj, G. (2022). Influence of pH and temperature parameters on the sol-gel synthesis process of meso porous ZrC nanopowder. *Ceramics International*, *48*(18), 26725-26731. <https://doi.org/10.1016/j.ceramint.2022.05.367>
- Norris, D. J., Efros, A. L., & Erwin, S. C. (2008). Doped nanocrystals. *Science*, *319*(5871), 1776-1779. <https://doi.org/10.1126/science.1143802>
- Novitasari, D., Lusiana, L. A., Sembiring, S., & Junaidi. (2022). Studi pendahuluan penentuan nilai energi band gap komposit perak silika (Ag/SiO₂) berbasis sekam padi [A preliminary study to determine the band gap energy value of silica silver composite (Ag/SiO₂) based on rice husk]. *Jurnal Teori dan Aplikasi Fisika*, *10*(1), 36-40. <https://doi.org/10.23960/jtaf.v10i1.2892>
- Nunes, P., Fortunato, E., Tonello, P., Fernandes, F. B., Vilarinho, P., & Martins, R. (2002). Effect of different dopant elements on the properties of ZnO thin films. *Vacuum*, *64*(3-4), 281-285. [https://doi.org/10.1016/S0042-207X\(01\)00322-0](https://doi.org/10.1016/S0042-207X(01)00322-0)
- Pandit, N. A., & Ahmad, T. (2022). Tin oxide based hybrid nanostructures for efficient gas sensing. *Molecules*, *27*(20), 7038. <https://doi.org/10.3390/molecules27207038>

- Patil, S. L., Sankapal, S. R., & Almunaser, F. M. A. (2023). Dip coating: Simple way of coating thin films. In B. R. Sankapal, A. Ennaoui, R. B. Gupta, & C. D. Lokhande (Eds.), *Simple chemical methods for thin film deposition: Synthesis and applications* (pp. 425-447). Springer. https://doi.org/10.1007/978-981-99-0961-2_10
- Paul David, S., Soosaimanickam, A., Sakthivel, T., Sambandam, B., & Sivaramalingam, A. (2021). Thin film metal oxides for displays and other optoelectronic applications. In S. Rajendran, J. Qin, F. Gracia, & E. Lichtfouse (Eds.), *Metal and metal oxides for energy and electronics* (pp. 185-250). Springer. https://doi.org/10.1007/978-3-030-53065-5_6
- Prastiwi, W. D., Maulana, K. D., Wibowo, E. A. P., Aji, N. R., & Setyani, A. (2017). Sintesis dan karakteristik TiO₂ dan SiO₂ serta aplikasinya terhadap kadar Fe dalam air sumur [Synthesis and characteristics of TiO₂ and SiO₂ and its application to Fe levels in well water]. *Jurnal Ilmiah Sains*, 17(1), 30-34. <https://doi.org/10.35799/jis.17.1.2017.15220>
- Preeti., & Rohilla, S. (2020). Rietveld refinement and structural characterization of TiO₂/CoFe₂O₄ nanocomposites. In *IOP Conference Series: Materials Science and Engineering* (Vol. 872, No. 1, p. 012171). IOP Publishing. <https://doi.org/10.1088/1757-899X/872/1/012171>
- Putra Parmita, A. W. Y. P., Panji., Sasongko, A., Qulub, F., & Triana, Y. (2023). Studi pengaruh temperatur kalsinasi dalam pembentukan nanomagnetite dengan metode green synthesis ekstrak daun nanas [Study of the influence of calcination temperature on the formation of nanomagnetite using the green synthesis method of pineapple leaf extract]. *SPECTA Journal of Technology*, 7(2), 584-592. <https://doi.org/10.35718/specta.v7i2.940>
- Rad, A. S., Afshar, A., & Azadeh, M. (2023). Antireflection and photocatalytic single layer and double layer ZnO and ZnO-TiO₂ thin films. *Optical Materials*, 136, 113501. <https://doi.org/10.1016/j.optmat.2023.113501>
- Rahmawati, E., & Agustina, S. (2018). Rekayasa permukaan lapisan tipis kitosan sebagai dasar pengembangan teknologi *self cleaning* [Surface engineering of a thin layer of chitosan as a basis for the development of self-cleaning technology]. *Gravity Edu: Jurnal Pembelajaran dan Pengajaran Fisika*, 1(2), 16-19. <https://doi.org/10.33627/ge.v2i2.95>
- Ramesh, K. S., Saravanabhavan, M., Muhammad, S., Edison, D., Ho, M.-S., Sekar, M., & Al-Sehemi, A. G. (2023). Synthesis, physico-chemical characterization and quantum chemical studies of 2, 3-dimethyl quinoxalium-5-sulphosalicylate crystal. *Journal of Molecular Structure*, 1285, 135425. <https://doi.org/10.1016/j.molstruc.2023.135425>
- Raub, A. A. M., Bahru, R., Nashruddin, S. N. A. M., & Yunas, J. (2024). A review on vertical aligned zinc oxide nanorods: Synthesis methods, properties, and applications. *Journal of Nanoparticle Research*, 26, 186. <https://doi.org/10.1007/s11051-024-06098-w>
- Ridhuan, N. S., Abdul Razak, K., Lockman, Z., & Abdul Aziz, A. (2012). Structural and morphology of ZnO nanorods synthesized using ZnO seeded growth hydrothermal method and its properties as UV sensing. *PLOS One*, 7(11), e50405. <https://doi.org/10.1371/journal.pone.0050405>
- Rizaldi, D. R., Doyan, A., & Susilawati, S. (2022). Sintesis lapisan tipis TiO₂:(F + In) pada substrat kaca dengan metode spin-coating sebagai bahan sel surya [Synthesis of a thin layer of TiO₂:(F + In) on a glass substrate using the spin-coating method as a solar cell material]. *ORBITA: Jurnal Pendidikan dan Ilmu Fisika*, 7(1), 219-224.

- Sahdiah, H., & Kurniawan, R. (2023). Optimasi tegangan akselerasi pada scanning electron microscope–energy dispersive X-ray spectroscopy (SEM-EDX) untuk pengamatan morfologi sampel biologi [Optimization of acceleration voltage on scanning electron microscope–energy dispersive X-ray spectroscopy (SEM-EDX) for observing the morphology of biological samples]. *Jurnal Sains dan Edukasi Sains*, 6(2), 117-123. <https://doi.org/10.24246/juses.v6i2p117-123>
- Santibenchakul, S., Sirijaturaporn, P., Mekprasart, W., & Pechrapa, W. (2018). Ga-doped ZnO nanoparticles synthesized by sonochemical-assisted process. *Materials Today: Proceedings*, 5(6), 13865-13869. <https://doi.org/10.1016/j.matpr.2018.02.030>
- Schell, J., Lupascu, D. C., Carbonari, A. W., Mansano, R. D., Dang, T. T., & Vianden, R. (2017). Implantation of cobalt in SnO₂ thin films studied by TDPAC. In *AIP Advances* (Vol. 7, No. 5, p. 055304). AIP Publishing. <https://doi.org/10.1063/1.4983270>
- Sharifi, F., Mahmoodi, Z., Abbasi, S. M., Najafi, A., & Khalaj, G. (2023). Synthesis and characterization of mesoporous TiC nanopowder/nanowhisker with low residual carbon processed by sol-gel method. *Journal of Materials Research and Technology*, 22, 2462-2472. <https://doi.org/10.1016/j.jmrt.2022.12.097>
- Silva, D. J., Barbosa, R. F. S., Souza, A. G., Ferreira, R. R., Camani, P. H., & Rosa, D. S. (2022). Morphological, UV blocking, and antimicrobial features of multifunctional cotton fibers coated with ZnO/Cu via sonochemistry. *Materials Chemistry and Physics*, 286, 126210. <https://doi.org/10.1016/j.matchemphys.2022.126210>
- Susilawati., & Doyan, A. (2009). Dose response and optical properties of dyed poly vinyl alcohol-trichloroacetic acid polymeric blends irradiated with gamma-rays. *American Journal of Applied Sciences*, 6(12), 2071-2077. <https://doi.org/10.3844/ajassp.2009.2071.2077>
- Tang, X., & Yan, X. (2017). Dip-coating for fibrous materials: Mechanism, methods and applications. *Journal of Sol-Gel Science and Technology*, 81, 378-404. <https://doi.org/10.1007/s10971-016-4197-7>
- Tarwal, N. L., & Patil, P. S. (2011). Enhanced photoelectrochemical performance of Ag–ZnO thin films synthesized by spray pyrolysis technique. *Electrochimica Acta*, 56(18), 6510-6516. <https://doi.org/10.1016/j.electacta.2011.05.001>
- Tjahjanti, P. H. (2019). *Pengetahuan bahan teknik* [Knowledge of technical materials]. Umsida Press. <https://doi.org/10.21070/2019/978-602-5914-85-0>
- Veerabhadraiah, S. R., Maji, S., & Panneerselvam, A. (2022). Solvent influence on the formation of ZnO nanoparticles by sonochemical technique and evaluation of UV-blocking efficiency. *Journal of Crystal Growth*, 579, 126430. <https://doi.org/10.1016/j.jcrysgro.2021.126430>
- Vyas, S. (2020). A short review on properties and applications of zinc oxide based thin films and devices: ZnO as a promising material for applications in electronics, optoelectronics, biomedical and sensors. *Johnson Matthey Technology Review*, 64(2), 202-218. <https://doi.org/10.1595/205651320X15694993568524>
- Woods-Robinson, R., Han, Y., Zhang, H., Ablekim, T., Khan, I., Persson, K. A., & Zakutayev, A. (2020). Wide band gap chalcogenide semiconductors. *Chemical Reviews*, 120(9), 4007-4055. <https://doi.org/10.1021/acs.chemrev.9b00600>

- Xian, G., Zhang, G., Chang, H., Zhang, Y., Zou, Z., & Li, X. (2019). Heterogeneous activation of persulfate by $\text{Co}_3\text{O}_4\text{-CeO}_2$ catalyst for diclofenac removal. *Journal of Environmental Management*, 234, 265-272. <https://doi.org/10.1016/j.jenvman.2019.01.013>
- Xin, N., Guan, J., Zhou, C., Chen, X., Gu, C., Li, Y., Ratner, M. A., Nitzan, A., Stoddart, J. F., & Guo, X. (2019). Concepts in the design and engineering of single-molecule electronic devices. *Nature Reviews Physics*, 1, 211-230. <https://doi.org/10.1038/s42254-019-0022-x>
- Yang, X., Yokokura, S., Nagahama, T., Yamaguchi, M., & Shimada, T. (2022). Molecular Dynamics simulation of poly (ether ether ketone) (PEEK) polymer to analyze intermolecular ordering by low wavenumber Raman spectroscopy and X-ray diffraction. *Polymers*, 14(24), 5406. <https://doi.org/10.3390/polym14245406>
- Yang, Y., Shen, L., Yuan, F., Fu, H., & Shan, W. (2018). Preparation of sustained release capsules by electrostatic dry powder coating, using traditional dip coating as reference. *International Journal of Pharmaceutics*, 543(1-2), 345-351. <https://doi.org/10.1016/j.ijpharm.2018.03.047>
- Yurestira, I., Aji, A. P., Desfri, M. F., Rini, A. S., & Rati, Y. (2021). Potensi ZnO/ZnS sebagai electron transport material pada sel surya perovskit [Potential of ZnO/ZnS as electron transport materials on perovskite solar cells]. *Journal of Aceh Physics Society*, 10(2), 41-47.
- Zaini, M. B., Maryam, S., Suryani, S. E. I., Himmah, S. W., Nurdiana, Z., Solehudin, S., Suprayogi, T., Sunaryono, S., & Diantoro, M. (2018). Pengaruh fraksi nano ($\text{TiO}_2\text{: SnO}_2$) terhadap struktur dan efisiensi DSSC $\text{TiO}_2\text{: SnO}_2/\beta\text{-karoten/FTO}$ [The effect of nano fraction ($\text{TiO}_2\text{: SnO}_2$) on the structure and efficiency of DSSC $\text{TiO}_2\text{: SnO}_2/\beta\text{-carotene/FTO}$]. *Journal of Physical Science and Engineering*, 3(2), 63-69. <https://doi.org/10.17977/um024v3i22018p063>
- Zhang, Q., Zhang, J., Cao, Y., Jiang, F., Feng, G., Liu, J., Liang, J., Li, H., Hu, Q., & Xu, Z. (2025). Low-temperature preparation of nano-sized Al_2TiO_5 powder via non-hydrolytic sol-gel route with Al metal as the aluminum source. *Journal of Alloys and Compounds*, 1010, 177716. <https://doi.org/10.1016/j.jallcom.2024.177716>
- Zhao, L., Jiang, Q., & Lian, J. (2008). Visible-light photocatalytic activity of nitrogen-doped TiO_2 thin film prepared by pulsed laser deposition. *Applied Surface Science*, 254(15), 4620-4625. <https://doi.org/10.1016/j.apsusc.2008.01.069>